**CSIRO** PUBLISHING

www.publish.csiro.au/journals/mfr *Marine and Freshwater Research*, 2005, **56**, 805–814

# Otolith shape feature extraction oriented to automatic classification with open distributed data

*J. Piera*[A,B,E], *V. Parisi-Baradad*[C], *E. García-Ladona*[D], *A. Lombarte*[D], *L. Recasens*[D] *and J. Cabestany*[C]

[A]Marine Technology Unit (CMIMA-CSIC), Passeig Marítim 37-49, Barcelona 08003, Catalonia, Spain.
[B]Signal Theory and Communications Department, Universitat Politècnica de Catalunya (UPC), Av Canal Olímpic s/n, Castelldefels 08860, Barcelona, Catalonia, Spain.
[C]Electronic Engineering Department, Universitat Politècnica de Catalunya (UPC), Gran Capità, s/n, module C4, Campus Nord. Barcelona 08034, Catalonia, Spain.
[D]Institut de Ciències del Mar (CMIMA-CSIC), Passeig Marítim 37-49, Barcelona 08003, Catalonia, Spain.
[E]Corresponding author. Email: jpiera@tsc.upc.es

*Abstract.* The present study reviewed some of the critical pre-processing steps required for otolith shape characterisation for automatic classification with heterogeneous distributed data. A common procedure for optimising automatic classification is to apply data pre-processing in order to reduce the dimension of vector inputs. One of the key aspects of these pre-processing methods is the type of codification method used for describing the otolith contour. Two types of codification methods (Cartesian and Polar) were evaluated, and the limitations (loss of information) and the benefits (invariance to affine transformations) associated with each method were pointed out. The comparative study was developed using four types of shape descriptors (morphological, statistical, spectral and multiscale), and focused on data codification techniques and their effects on extracting shape features for automatic classification. A new method derived from the Karhunen–Loève transformation was proposed as the main procedure for standardising the codification of the otolith contours.

*Extra keywords*: image processing, shape characterisation, shape descriptors.

## Introduction

Sagittal otoliths are characterised by a high morphological variability (Platt and Popper 1981). Their shape has a specific form and has been used to identify species (Schmidt 1969) and populations (Messieh 1972), as well as being applied in taxonomical (Nolf 1985), phytogenetical (Gaemers 1976), palaeontological (Schwarzhans 1980), and food web studies (Frost and Lowry 1981). The development of image processing systems has been essential for the development of quantitative methods to describe otolith shapes (Castonguay *et al*. 1991; Lombarte and Castellón 1991). However, by using image analysis to characterise otolith shapes represents a challenging and important problem in automatic classification.

In recent years, the development of new scientific networking technologies has provided remote access to distributed data from different resources (Cornillon *et al*. 2003). In the case of otolith research, access to different collections of otolith images has opened the possibility of new characterisation and classification methods based on global and larger otolith shape datasets (Chic *et al*. 2004).

In this new potential framework of data analysis, it is important to define the general processes for characterising the otolith images. In general, there are two approaches to otolith shape characterisation: region-based, which deals with the region in the image corresponding to the analysed otolith; and boundary based, where the shape is analysed in terms of its silhouette (Pavlidis 1977). Whereas the former is intrinsically a bidimensional (2D) analysis, dealing directly with planar primitives and concepts, the latter can transform the bidimensional operations through the unidimensional representation of the silhouette; we refer to it henceforth as contour characterisation. This second option is used widely because the input data dimension is highly reduced, the instrumental requirements for contour acquisition are lower than those required for the complete image, and most of the important features of the otolith image can be obtained from its contour.

Contour characterisation is based on two main processes: first, it is necessary to compute a mathematical representation of the contour shape (contour extraction) and second a set of different descriptors is computed from this contour representation (feature extraction).

 10.1071/MF04163 1323-1650/05/050805

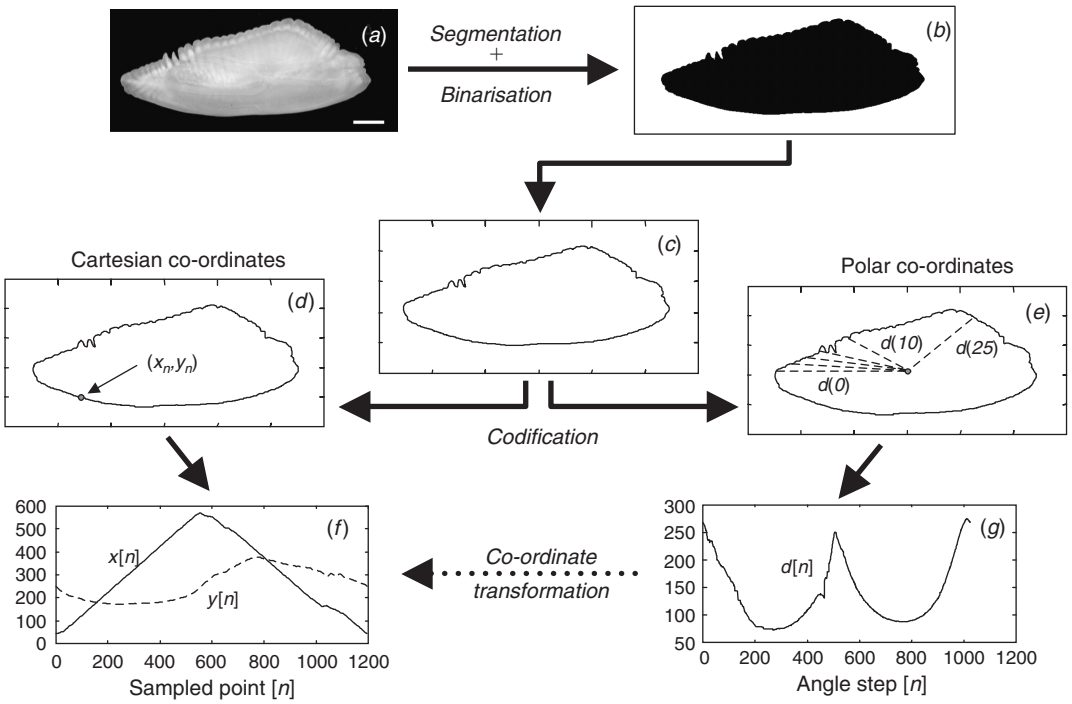


**Fig. 1.** Schematic diagram of the different steps required for computing the contour codification.

Extracting the contour from the original otolith image involves different steps (Fig. 1). The first consists of separating the otolith from other image structures (segmentation) followed by making a representation of its silhouette (binarisation). The second step consists of extracting the boundary points of the silhouette and then tracking the boundary from an initial point (codification). This process leads to a linearised list of points, which depends on the selected initial point and the form used for co-ordinate codification. Examples of different types of codification are the direct form of pair-co-ordinates $(x[n], y[n])$, using two real numbers for each point, or the complex formulation $x[n] + j \cdot y[n]$ (where $j = \sqrt{-1}$) which requires a single complex value for each contour point.

Which features are chosen to classify the different contours is particularly critical, because it can have a significant impact on the final result. Indeed, the process of choosing suitable features has often been identified as a more critical step than choosing the classification algorithms (Ripley 1996).

Although feature selection has been considered to be one of the key aspects for automatic classification, it is important to note that several features, some of them potentially discriminant, are dependent on the selected contour extraction process. This problem was not relevant in previous studies involving otolith shape where the method for contour extraction was developed following the uniform criteria selected by the authors. However, owing to the possibility of analysing otolith datasets from different resources, it is important to find general methods that can be applied to contours obtained with different contour extraction and codification procedures.

This paper investigates to what extent several critical points of this process affect the capacity to discriminate the otolith shape, by using different types of morphological, statistical, spectral and multiscale contour descriptors as a reference.

## Material and methods

### *Otolith orientation methods*

In previous studies, the orientation of the otolith was standardised according to different morphological criteria (Lombarte and Lleonart 1993; Campana and Casselman 1993; Cadrin and Friedland 1999; Cardinale *et al*. 2004). In automatic recognition of otoliths obtained from different sources, it is important to define objective (mathematical) criteria for defining the orientation of the otolith contour.

A good candidate method for standardising contour orientation is the Hotelling or Karhunen–Loève (KL) transformation (Hotelling 1933; Karhunen 1946; Loève 1955), which is the mathematical basis of the empirical orthogonal functions (EOF) and principal component analysis (PCA). In this method, the covariance matrix of the co-ordinates is estimated and its respective Eigenvectors are then used to define a new linear transformation. This transformation minimises the covariance of the new co-ordinates becoming perfectly uncorrelated. Depending on the original orientation of the otolith, there are only two possible solutions in which the co-ordinates are uncorrelated and the variance is maximised along the *x*-axis. The human interaction is reduced to selecting from these two possible representations. The advantage of this method is that it provides an objective method for orienting the otolith contour,

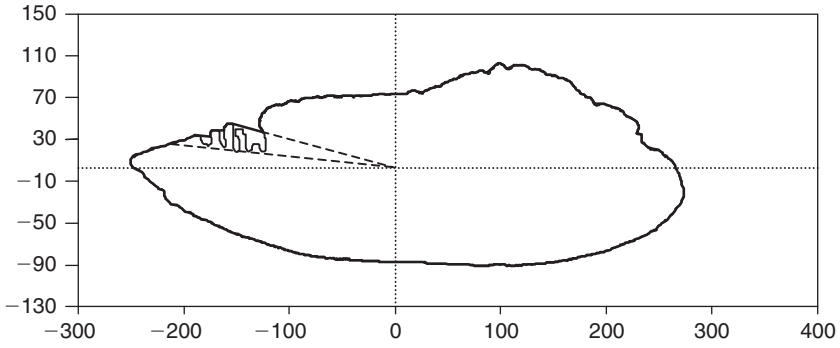


**Fig. 2.** Comparison of the contours obtained with Cartesian co-ordinates (in black) and the reconstructed contours from Polar codification, showing the limitations of the reconstruction.

while providing the possibility of extracting different features from the uncorrelated co-ordinates.

*Contour codification*

In the present study, two types of contour codification have been analysed: Cartesian, both in the direct ($x[n], y[n]$) and complex ($x[n]+j \cdot y[n]$) form, and Polar ($\rho[\theta]$). Although there are many alternative codification methods, such as polynomic approximations (Ramer 1972; Pavlidis 1973; Pavlidis and Horowitz 1974), electrical charge distributions (Wu and Levine 1995), and non-linear algorithms (Zhu and Chirlian 1995), the analysis has been restricted to those mentioned earlier, as they are the most widely used in otolith research.

The main advantage of Polar codification is that it is possible to obtain a one-dimensional representation of the contour, simplifying the shape characterisation process. Another advantage is that there is a direct conversion between Polar and Cartesian codifications

$$x[n] = \rho[n] \cdot \cos(\theta[n])$$
$$y[n] = \rho[n] \cdot \sin(\theta[n])$$

The conversion from Polar to Cartesian co-ordinates is important in the cases that need to analyse data with heterogeneous codification from different resources. However, as shown in the example in Fig. 2, reconstructing the original shape from its Polar codification has some limitations, especially in the cases where the otolith shape is complex with conspicuous inclusions.

*Feature selection for automatic classification*

The design of a pattern classifier requires selecting a set of features that best discriminate the pattern classes. The final performance of the classification will depend on the classification algorithms selected. This is a very difficult task for automatic classification as in many cases it depends on the specific problem domain (Costa and Cesar 2002).

In order to simplify the analysis of the effects of the pre-processing procedures, the features have been selected *a priori*, trying to cover the maximum range of feature types. Four shape descriptor classes were selected from among the most classical classes within otolith research: morphological based, statistical (including fractal dimension), Fourier descriptors and multiscale based. The potential performance of the classification based on a single feature was evaluated by using the class separation distance (Castelman 1996). With this parameter, it is possible to evaluate the capability of discriminating two different classes using a selected feature. If we have $n$ different classes characterised with $m$ different features, the class separation distance (CSD) between the $l$ and $k$ classes with respect to the $m$-th feature is defined as:

$$CSD_{l,k,m} = \frac{|\mu_{l,m} - \mu_{k,m}|}{\sqrt{\alpha_{l,m}^2 + \alpha_{k,m}^2}}$$

where $\mu$ and $\sigma^2$ represent the mean and the variance of the $m$-th feature computed by using the samples associated with the $l$ and $k$ classes (indicated with the corresponding subindex). The discrimination capabilities of the selected feature increases with $CSD_{l,k,m}$. The objective of the present analysis is to determine which pre-processing procedures maximise the class separation distance using the selected features as a reference framework.

*Morphological-based shape descriptors*

The first selected set of features corresponds to general morphological descriptors.

*Perimeter*

The arc length of the contour can be estimated by using different approaches, depending on the type of codification (Costa and Cesar 2002). In direct co-ordinates it can be computed as:

$$P = \sum_{n=0}^{N-1} d(n,n-1)$$

where

$$d(n,n-1) = \sqrt{(x[n] - x[n-1])^2 + (y[n] - y[n-1])^2}$$

and $d(0,-1) = d(0,N-1)$. In the case of complex codification $u[n] = x[n] + j \cdot y[n]$,

$$P = \sum_{n=0}^{N-1} |u[n] - u[n-1]|$$

where $u[-1] = u[N-1]$ and $|u[n]|$ denotes the complex modulus.

*Maximum chord*

This is defined as the line segment joining the furthest points within the contour. Taking into account the normalised orientation of the contour, it is possible to derive different features from this line: the co-ordinates ($x_{mc0}$, $y_{mc0}$, $x_{mc1}$, $y_{mc1}$) and the modulus ($Mc$).

*Major and minor axes*

The Hotteling transform provides the Eigen values of the contour co-ordinates, which can be considered as additional morphological descriptors. The major axis and minor axis are associated with the maximum and minimum Eigen values.

*Morphological ratios*

Additional features can be computed between ratios of the features defined above (Costa and Cesar 2002), such as the ratio between the major and minor axis (known as the *aspect ratio*), the ratio between the major axis and the perimeter and the ratio between the major axis and the maximum chord.

*Statistical and fractal shape descriptors*

*Mean and variance co-ordinates*

Given the method for standardising the contour orientation, four value types of mean and variance co-ordinates were evaluated. The first type of statistical descriptor was global variance, which was computed considering all the contour co-ordinates. Alternatively, different mean and variances were estimated considering only subsets of contour co-ordinates. Upward mean and upward variance were computed from co-ordinates with positive ordinates ($y[n] \geq 0$). Following a similar subset selection, different mean and variances were defined: downward mean and variance (from co-ordinates with $y[n] < 0$), right mean and variance (co-ordinates with $x[n] \geq 0$) and left mean and variance (co-ordinates with $x[n] < 0$). Finally, different ratios from these descriptors were also computed: upward–downward and right–left.

*Fractal dimension*

The fractal dimension of the otolith contours was also considered, as fractal measures have been applied widely to different problems in image processing analysis and pattern recognition (Peitgen and Saupe 1998). The fractal dimension was computed by using the box counting algorithm. This method is based on partitioning the shape image into square boxes of size L × L and counting the number of boxes ($n$(L)) containing a portion of the shape. By varying the box size L, the fractal dimension is calculated as the absolute value of the slope of the line obtained from the linear regression of the (log(L), log($n$(L))) curve (Fig. 3).

*Fourier shape descriptors*

The mathematical background underlying the Fourier analysis theory provides a large set of useful tools for shape analysis. In the present analysis, the Fourier descriptors proposed by Granlund (1972) are considered, as they are one of the most popular shape representation methods for vision and pattern recognition applications.

$$FD(s) = \sum_{n=0}^{N-1} u(n) e^{-j2\pi ns/N}, \quad s = 0, \ldots, N-1$$

Shen *et al*. (1994) proposed a normalised version of Fourier descriptors:

$$NFD(s) \begin{cases} 0; & s = 0 \\ |FD(s)/FD(1)|; & s \neq 0 \end{cases}$$

The normalised Fourier descriptors are invariant to translation, rotation, parameter shifting and scaling. In the present study, however, it is not necessary to compute the normalised descriptors, because the proposed standardisation method based on K–L transformation provides also the invariant property.

*Curvature-based shape descriptors*

The multiscale descriptor selected is based on the curvature estimation at different scales. The curvature is one of the most important features that can be extracted from contours. Formally, the curvature $k(t)$ of a contour shape ($x(t)$, $y(t)$) is defined as:

$$k(t) = \frac{\dot{x}(t)\ddot{y}(t) - \ddot{x}(t)\dot{y}(t)}{(\dot{x}(t)^2 + \dot{y}(t)^2)^{3/2}}$$

where the upper dot and double dot represent the first and second derivative respectively. The problem of estimating the derivatives of $x(t)$ and $y(t)$ in computational shape analysis, where the contour is represented in discrete co-ordinates, can be solved with different approaches. In the present study, the discrete values of the curvature were computed by using the derivative properties of the Fourier Transform (Papoulis 1962) combined with a formula from differential geometry (do Carmo 1976).

*Bending energy*

One of the most important curvature-based measures related to shape complexity is bending energy (Young *et al*. 1974). This global feature is defined in a discrete form as:

$$B = \frac{1}{N} \sum_{n=0}^{N-1} k[n]^2$$

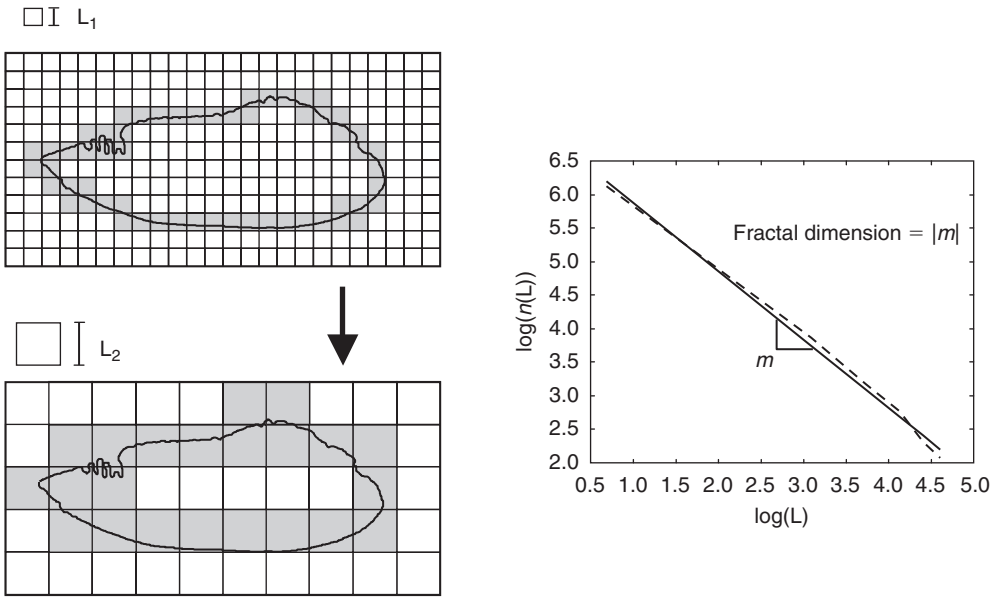


**Fig. 3.** Illustration of the box-counting method for estimating the fractal dimension of the otolith contour.

where $n$ is the total number of contour points. This measure, inspired from elasticity theory, expresses the amount of energy needed to transform a closed contour into a circle with the same perimeter as the original one.

*Multiscale bending energy*

Curvature estimation is sensitive to noise and discretisation errors because signal differentiation acts as a high pass filter that accentuates the influence of high frequency noise. Introducing a low-pass filter in the derivative estimation step can control this undesirable effect. A common practice is to combine the Fourier-based numerical differentiation process with a Gaussian low-pass filter, adjusting the bandwidth of the filter using the Gaussian standard deviation, $a$ (Costa and Cesar 2002). By using different values of the standard deviation, $a$ (also known as *scale* factor in this context), it is possible to define a series of smoothed versions of the original contour. Several scale-dependent curvature descriptors can be computed from this family of curves. In the present study, the otolith contours were characterised with the normalised multiscale bending energy (NMBE) defined as:

$$NMBE[a] = \frac{P^2}{N} \sum_{n=0}^{N-1} k[a,n]^2$$

Figure 4 shows an example of the graphical evolution of the generated contours, known as morphograms (Cesar and Costa 1997), and its associated NMBE values at different scales.

*Description of the matrix features*

Four different feature matrices were computed according to the feature classes: morphological, fractal and statistical, spectral (Fourier descriptors) and multiscale (bending energy).

- *Morphological*. 11 features: perimeter, max. chord, co-ordinates max. chord (×4), major-axis, minor-axis, aspect ratio (major-axis/minor-axis), max. chord/perimeter.
- *Fractal and statistical*. 27 features: fractal dimension, total variance (×2), upward–downward mean and variance (×4), right–left mean and variance (×4), and the corresponding rations (×16).
- *Fourier descriptors*. 256 features: 256 Fourier components.
- *Multiscale*. 64 features: normalised multiscale bending energy computed at 64 different scales. The scales were selected within the interval ($10^{-0.8}$–$10^{-0.7}$), using logarithmically equally spaced criteria to obtain the different scale values.

*Otolith dataset*

The otolith dataset selected for evaluation purposes was obtained from a collection of European hake, *Merluccius merluccius* (L.), from biological sampling performed monthly between September 1989 and June 1991 in the Mediterranean Sea (Recasens *et al*. 1998).

Following on from the study conducted by Recasens *et al*. (1998), six different classes were defined according to the criteria of sex, maturity and length. Table 1 summarises the features associated with each class.

**Table 1. Features associated with the otolith dataset classes of European hake *Merluccius merluccius* (L.) used to evaluate the differences in contour classification**

| Class | Sex | Maturity stage | Length | No. samples |
|---|---|---|---|---|
| I | Undetermined | Juvenile, 1st year | <16 cm | 24 |
| II | Male | Juvenile, after 1st year | (16–28.8) cm | 18 |
| III | Female | Juvenile, after 1st year | (16–38.0) cm | 25 |
| IV | Male | Adult | >28 cm | 23 |
| V | Female | Adult | (38.0–60.0) cm | 31 |
| VI | Female | Adult | >60 cm | 9 |

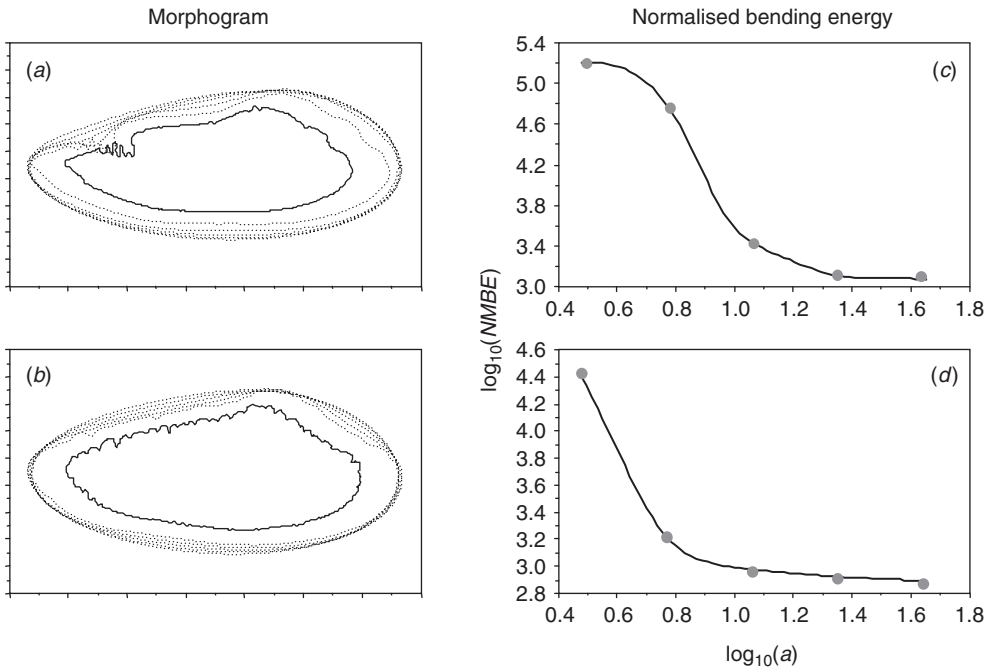


**Fig. 4.** (*a*,*b*) Example of the morphograms computed from two different contour morphologies. (*c*,*d*) The different features of these contours can be appreciated in their respective normalised multiscale bending energy (NMBE) curves.

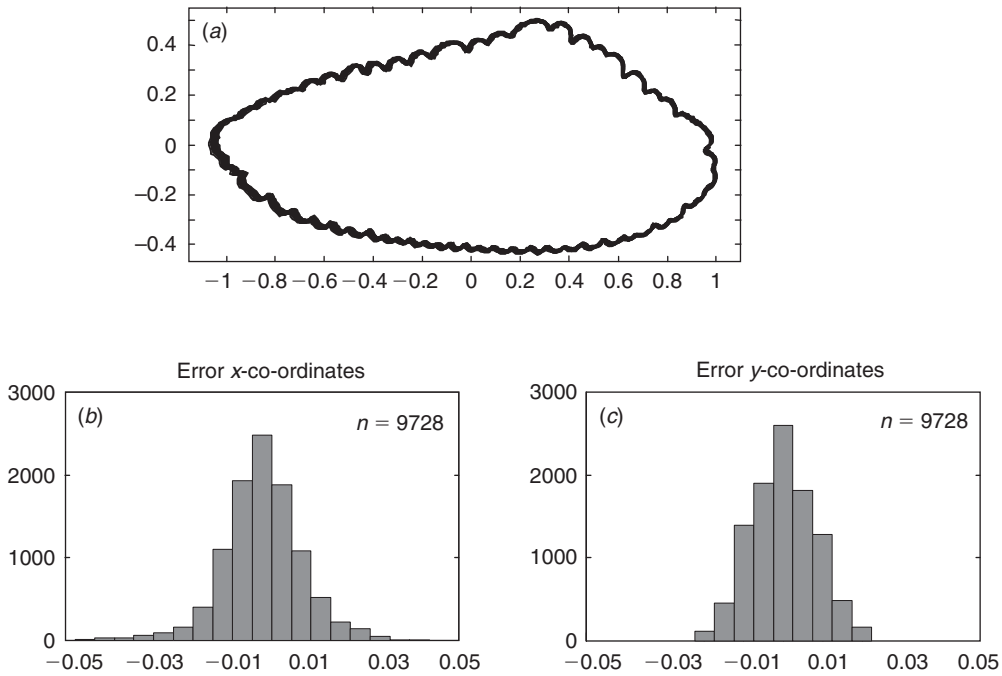


**Fig. 5.** (*a*) Overlapped contours obtained in the test of the orientation standardisation method. (*b*,*c*) Histograms of the differences between the contour co-ordinates (in grey) and the contour reference (in black).

## Results

### *Otolith co-ordinate standardisation*

The first objective was to evaluate a KL-transform-derived method as a tool for obtaining a final contour codification that does not vary according to the position and orientation of the original shape. A set of 20 images of the same otolith with different orientations and resolutions (images from $140 \times 190$ up to $780 \times 780$ pixels), was obtained to test the method. The orientation of the different images was standardised by using an automatic algorithm that applies the KL-transform, and an interactive programme to check this orientation. An automatic procedure computed the same origin reference ($x > 0,\ y = 0$) for each image, and then a total of 512 points were obtained interpolating the original contour co-ordinates. As different image resolutions yield different co-ordinate values, it was necessary to normalise the co-ordinates. For this purpose, the interpolated points were normalised to $(x[n],y[n])' = (x[n]/\max(x[n]),y[n]/\max(x[n]))$.

From this set of normalised contours, the error position of 9728 co-ordinate-pairs was evaluated. The reference contour was obtained from the highest resolution image. Figure 5 shows the graphical result of overlapping the 20 different normalised contours and the histograms corresponding to errors in *x*-co-ordinates (90% error confidence interval (−0.0156, 0.0165)) and *y*-co-ordinates (90% confidence interval (−0.0127, 0.0136)). Taking into account the normalised process, the error intervals indicate that the co-ordinate errors can be considered to be below 1% of the full scale.

### *Comparing the discriminant capacity using Cartesian and Polar codification*

Two different sets of feature matrices were obtained by using Cartesian and Polar contour codification. The effect of choosing different types of codification methods could be seen in many features, as shown in Fig. 6, where the information lost in relation to shape inclusions, resulted in lower normalised multiscale bending energy values.

The class separation distance (CSD) was obtained for all features and classes yielding a total of 358 ($6 \times 6$) square matrices. Statistics (mean, maximum and minimum CSD values) were computed for each matrix in order to determine the features with the highest potential for discrimination. In general, the features obtained from the Polar converted co-ordinates had higher associated CSD values. This trend can be observed in the plots in Fig. 7, in which the minimum, maximum and mean CSD values are represented for all the feature types. In order to simplify the visual comparison, the features were sorted, obtaining a monotonic increasing curve for the mean CSD values associated with the Cartesian codification.

Table 2 summarises the differences obtained in Fig. 7, identifying for each type of shape descriptor, the parameters with the highest potential to be used for discrimination purposes. In each case, the three descriptors with the highest mean CSD values were included.

## Discussion

One of the surprising results is that, although information is lost in Polar codification, the higher associated CSD values

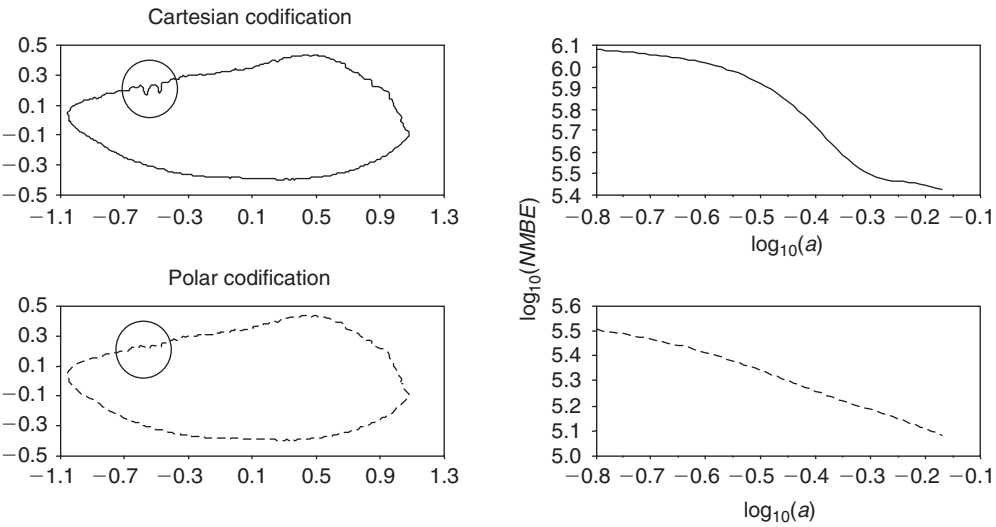


**Fig. 6.** Example of the differences in the normalised multiscale bending energy (NMBE) estimated from the two codification methods.

**Table 2. Summary of the class separation distance (CSD) values obtained with Cartesian and Polar converted co-ordinates**
The table includes the features with the highest mean CSD values computed from the four feature types

| | Cartesian codification | | Polar codification | |
|---|---|---|---|---|
| Morphological feature | Aspect ratio | 0.783 | Aspect ratio | 1.036 |
| | Max. chord/perimeter | 0.663 | Max. chord/perimeter | 1.027 |
| | Major axis | 0.656 | Perimeter | 0.772 |
| Fractal and statistical | Variance downward *y*-co-ordinate | 0.928 | Variance downward *y*-co-ordinate | 0.926 |
| | Mean downward *y*-co-ordinate | 0.780 | Mean downward *y*-co-ordinate | 0.886 |
| | Mean upward *x*-co-ordinate | 0.738 | Variance right *x*-co-ordinate | 0.787 |
| Spectral (Fourier descriptors) | FD5 | 0.589 | FD4 | 0.8116 |
| | FD44 | 0.580 | FD1 | 0.7964 |
| | FD42 | 0.562 | FD2 | 0.6429 |
| Multiscale (normalised multiscale bending energy) | NBE64 | 0.638 | NBE62 | 0.773 |
| | NBE63 | 0.637 | NBE63 | 0.771 |
| | NBE62 | 0.634 | NBE61 | 0.767 |

seem to indicate that this codification method could be better than the Cartesian method for classification purposes.

However, the CSD is a relatively simple parameter that has been used to evaluate the potential discrimination capacity of a single parameter and compare different codification methods. It is also important to note that this improvement does not allow us to use a single feature for classification, as in most cases, the minimum CSD is nearly zero, indicating its low capacity for discriminating some classes. It has been shown in many studies (Cardinale *et al*. 2004) that otolith classification is a difficult task that requires complex statistical tools and the combination of several features.

In order to evaluate the effect of using different codification methods with more complex statistical techniques, a linear discriminant function (Rao 1973) was performed. Tables 3 and 4 summarise the numerical results obtained with the Cartesian and Polar codification methods. The results show that discriminant analysis with Cartesian co-ordinate contours provide better results (90% of the total correct classifications) than the analysis performed with Polar co-ordinates (88.46% of the total correct classifications).

The discriminant analysis was also performed by using only Fourier descriptors, as they are the most popular features in the field of otolith research. This second comparison was performed in order to evaluate the benefits of including new descriptors in otolith classification. In this second analysis, and for both codification methods, the total of correct classifications was lower (87.69% for Cartesian co-ordinates, and 86.92% for Polar co-ordinates). The differences from the first analysis indicate that the alternative descriptors presented in the present study provide new capabilities for classification.

### *Future applications*

Distributed open data are emergent resources that can be very useful in future otolith research. When using otoliths from

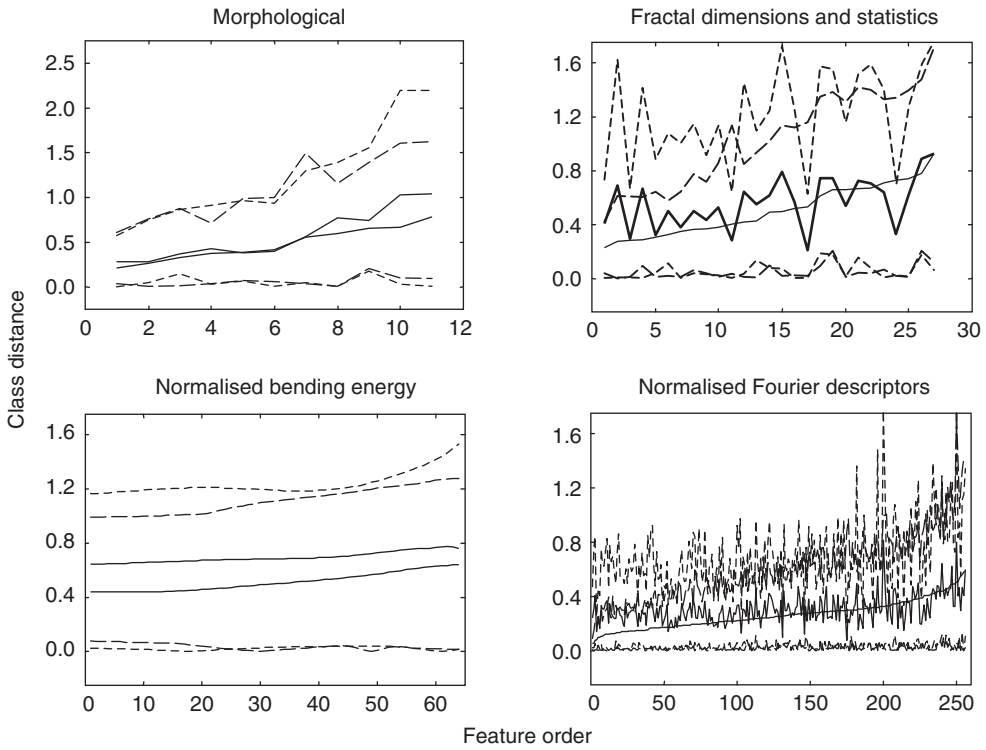


**Fig. 7.** Comparative results of the class separation distance (CSD) values (minimum, maximum and mean) obtained from the different feature types.

**Table 3. Classification results obtained with linear discriminant analysis using Cartesian co-ordinates**
Wilks' λ: 0.00613 approx. $F$ (270,359) = 2.3691, $P < 0.0000$

| | Percentage correct | Class I $P = 0.185$ | Class II $P = 0.138$ | Class III $P = 0.192$ | Class IV $P = 0.177$ | Class V $P = 0.238$ | Class VI $P = 0.069$ |
|---|---|---|---|---|---|---|---|
| Class I | 100.00 | 24 | 0 | 0 | 0 | 0 | 0 |
| Class II | 83.33 | 1 | 15 | 2 | 0 | 0 | 0 |
| Class III | 88.00 | 0 | 2 | 22 | 1 | 0 | 0 |
| Class IV | 91.30 | 0 | 0 | 1 | 21 | 1 | 0 |
| Class V | 90.32 | 0 | 0 | 0 | 3 | 28 | 0 |
| Class VI | 77.78 | 0 | 0 | 0 | 1 | 1 | 7 |
| Total | 90.00 | 25 | 17 | 25 | 26 | 30 | 7 |

**Table 4. Classification results obtained with linear discriminant analysis using Polar co-ordinates**
Wilks' λ: 0.00984 approx. $F$ (270,359) = 2.0337, $P < 0.0000$

| | Percentage correct | Class I $P = 0.185$ | Class II $P = 0.138$ | Class III $P = 0.192$ | Class IV $P = 0.177$ | Class V $P = 0.238$ | Class VI $P = 0.069$ |
|---|---|---|---|---|---|---|---|
| Class I | 100.00 | 24 | 0 | 0 | 0 | 0 | 0 |
| Class II | 88.89 | 1 | 16 | 0 | 1 | 0 | 0 |
| Class III | 92.00 | 0 | 1 | 23 | 1 | 0 | 0 |
| Class IV | 73.91 | 0 | 1 | 2 | 17 | 3 | 0 |
| Class V | 90.32 | 0 | 0 | 0 | 2 | 28 | 1 |
| Class VI | 77.78 | 0 | 0 | 0 | 0 | 2 | 7 |
| Total | 88.46 | 25 | 18 | 25 | 21 | 33 | 8 |

different databases, the differences in otolith contour description can be a potential problem for comparing their respective features. Neither otolith orientation nor image resolution is a serious problem as it is possible to compute normalised positions with relatively low error using the method proposed here. However, data conversion from different codification methods may affect the final result. In this sense, it is necessary to establish some type of standard format that allows the use of distributed data as a regular procedure.

Establishing a standard data format for otolith images could be one of the most important issues for future applications facilitating the exchange of data between different otolith databases. New descriptors can be developed to improve automatic classification methods. One type of promising descriptor is based on local singularities of the contour. These singularities can be related to landmark selection defined by expert taxonomists, who manually obtain morphological features for classification. Signal processing techniques related to local characterisation, such as Wavelet Transform and Curvature Scale Space representation (Parisi-Baradad *et al.* 2005) could provide these descriptors. The presence and position of particular singularities can be one of the most important sources of otolith characterisation. These singularities can be characterised by the Lipschitz–Hölder exponent, a parameter related to local regularity that can be obtained from Wavelet Transform (Jaffard 1992).

The possibility of normalising the otolith contour position provides additional advantages for this type of technique. It facilitates the comparison of the singularities between different contours and creates the possibility of developing new methods of fast automatic classification based on detecting contour singularities.

## Acknowledgments

The present study was funded by the IBACS project (European Union Project QLRT-2001-01610), by the Spanish project AVG-ION (McyT-TIC2000-0376-p4-04) from the Spanish Ministry of Science and Technology and by the IBACS European project. We would like to thank Antoni Cruz for his contribution in acquiring some of the otolith images processed, and Albert Martí for developing some of the required function routines. Remarks by two anonymous reviewers led to substantial improvements in the manuscript; they are thanked for their careful and constructive comments.

## References

Cadrin, S. X., and Friedland, K. D. (1999). The utility of image processing techniques for morphometric analysis and stock identification. *Fisheries Research* **43**, 129–139. doi:101016/S0165-7836(99)00070-3

Campana, S. E., and Casselman, J. M. (1993). Stock discrimination using otolith shape analysis. *Canadian Journal of Fisheries and Aquatic Sciences* **50**, 1062–1083.

Castelman, K. R. (1996). 'Digital Image Processing.' (Prentice Hall: Englewood Cliffs, NJ.)

Cardinale, M., Doering-Arjes, P., Kastowsky, M., and Mosegaard, H. (2004). Effects of sex, stock, and environment on the shape of known-age Atlantic cod (*Gadus morhua*) otoliths. *Canadian Journal of Fisheries and Aquatic Sciences* **61**, 158–167. doi:10.1139/F03-151

Castonguay, M., Simard, P., and Gagnon, P. (1991). Usefulness of Fourier analysis of otolith shape for Atlantic mackerel (*Scomber scombrus*) stock discrimination. *Canadian Journal of Fisheries and Aquatic Sciences* **48**, 296–302.

Chic, O., Cruz, A., Lombarte, A., Olivella, R., García-Ladona, E., Parisi, V., and Graña, M. (2004). AFORO: An interactive shape analysis and classification system for fish otoliths. In 'Abstracts of the 3rd International Symposium on Fish Otolith Research and Application, 11–16 July, 2004, Townsville'. p. 96. [Abstract]

Cornillon, P., Gallagher, J., and Sgouros, T. (2003). Opendap: accessing data in a distributed, heterogeneous environment. *Data Science Journal* **2**, 164–174.

Cesar, R. M., and Costa, L. F. (1997). Application and assessment of multiscale bending energy for morphometric characterization of neural cells. *Review of Scientific Instruments* **68**, 2177–2186. doi:10.1063/1.1148112

Costa, L. F., and Cesar, R. M. (2002). 'Shape Analysis and Classification. Theory and Practice.' (CRC Press: New York.)

do Carmo, M. P. (1976). 'Differential Geometry of Curves and Surfaces.' (Prentice-Hall: Englewood Cliffs, NJ.)

Frost, K. J., and Lowry, U. F. (1981). Trophic importance of some marine gadids in Northern Alaska and their body-otolith size relationships. *U.S. Fishery Bulletin* **79**, 187–192.

Gaemers, P. A. M. (1976). New concepts in the evolution of the Gadidae (Vertebrata, Pisces), based on their otoliths. *Mededelingen van de Werkgroep voor tertiare en kwartaire Geologie* **13**, 3–32.

Granlund, G. H. (1972). Fourier processing for hand print character recognition. *IEEE Transactions of Computers Institute of Electrical and Electronic Engineers* **21**, 195–201.

Karhunen, K. (1946). Zur Spektraltheorie Stochastischer Prozesse. Suomalainen Tiedeakatemia Toimituksia. Sar. A.4. *Biologica* **37**, 1–37.

Hotelling, H. (1933). Analysis of complex statistical variables into principal components. *Journal of Educational Psychology* **24**, 498–520.

Jaffard, S. (1992). Pointwise smoothness, two-microlocalization and wavelets coefficients. *Publicacions Matemàtiques* **35**, 155–168.

Loève, M. M. (1955). 'Probability Theory.' (VanNostrand: Princeton, NJ.)

Lombarte, A., and Castellón, A. (1991). Interespecific and intraspecific otolith variability in the genus *Merluccius* as determined by image analysis. *Canadian Journal of Zoology* **69**, 2442–2449.

Lombarte, A., and Lleonart, J. (1993). Otolith size changes related with body growth, habitat depth and temperature. *Environmental Biology of Fishes* **37**, 297–306.

Messieh, S. (1972). Use of otoliths in identifying herring stocks in the southern Gulf of St. Lawrence and adjacent waters. *Journal of the Fisheries Research Board of Canada* **29**, 1113–1118.

Nolf, D. (1985). Otolith piscium. In 'Handbook of Paleoichthyology, Vol. 10'. (Ed. H. P. Schultze.) pp. 1–145. (Gustav Fisher Verlag: Jena, Germany.)

Papoulis, A. (1962). 'The Fourier Integral and its Applications.' (McGraw-Hill: New York.)

Parisi-Baradad, V., Lombarte, A., Garcia-Ladona, E., Cabestany, J., Piera, J., and Chic, O. (2005). Otolith shape contour analysis using affine transformation invariant wavelet transforms and curvature scale space representation. *Marine and Freshwater Research* **56**, 795–804. doi:10.1071/MF04162

Pavlidis, T. (1973). Waveform segmentation through functional approximation. *IEEE Transactions on Computers. Institute of Electrical and Electronics Engineers* **7**, 689–697.

Pavlidis, T. (1977). 'Structural Pattern Recognition.' (Springer: New York.)

Pavlidis, T., and Horowitz, S. L. (1974). Segmentation of plane curves. *IEEE Transactions on Computers. Institute of Electrical and Electronics Engineers* **8**, 860–870.

Peitgen, H. O., and Saupe, D. (1998). 'The Science of Fractal Images.' (Springer: New York.)

Platt, C., and Popper, A. N. (1981). Fine structure and function of the ear. In 'Hearing and Sound Communication in Fishes'. (Eds W. N. Tavolga, A. N. Popper and R. R. Fay.) pp. 3–38. (Springer-Verlag: New York.)

Rao, C. R. (1973). 'Linear Statistical Inference and its Applications.' (J. Wiley and Sons: New York.)

Ramer, U. (1972). An iterative procedure for the polygonal approximation of plane curves. *Computer Graphics and Image Processing* **1**, 244–256.

Recasens, L., Lombarte, A., Morales-Nin, B., and Torres, G. (1998). Spatiotemporal variation in the population structure of the European hake in the NW Mediterranean. *Journal of Fish Biology* **53**, 387–401.

Ripley, B. D. (1996). 'Pattern Recognition and Neural Networks.' (Cambridge University Press: Cambridge, UK.)

Schmidt, W. (1969). The otoliths as a means for differentiation between species of fish of very similar appearance. In 'Proceedings of the Symposium on the Oceanogrophy and Fisheries Resources of the Tropical Atlantic, UNESCO, FAO and OAU'. pp. 393–396.

Schwarzhans, W. (1980). Die tertiäre Teleosteer-Fauna Neuseelands, rekonstruiert amhand von otolithen. *Berliner Geowissenschaftliche abhandlungen* **26**, 1–211.

Shen, L., Rangayyan, R. M., and Desautels, J. E. L. (1994). Application of shape analysis to mammographic calcifications. *IEEE Transactions on Medical Imaging* **13**, 263–274. doi:10.1109/42.293919

Young, I. T., Walker, J. E., and Bowie, J. E. (1974). An analysis technique for biological shape. *Information and Control* **25**, 357–370. doi:10.1016/S0019-9958(74)91038-9

Wu, K., and Levine, M. D. (1995). 2-D Shape segmentation: a new approach. Technical Report TR-CIM-95-01. Centre for Intelligent Machines, McGill University, Montreal.

Zhu, P., and Chirlian, P. M. (1995). On critical point detection of digital shapes. *IEEE Transactions on Pattern Analysis and Machine Intelligence* **17**, 737–748. doi:10.1109/34.400564

Manuscript received 16 July 2004; revised 17 February 2005; and accepted 11 March 2005.